# Power-efficient heterodyne radio over fiber link with laser phase noise robustness

**Yuancheng Cai (蔡沅成), Xiang Gao (高 翔), Yun Ling (凌 云)*, Bo Xu (许 渤), and Kun Qiu (邱 昆)**

*Key Laboratory of Optical Fiber Sensing and Communications, Ministry of Education, University of Electronic Science and Technology of China, Chengdu 611731, China*

**Corresponding author: yling@uestc.edu.cn*

Received May 8, 2019; accepted June 20, 2019; posted online September 4, 2019

A pre-coding-assisted power detection scheme for radio over fiber downlink is presented. This scheme can eliminate laser phase noise while avoiding high energy-consuming electrical carrier required in conventional power and/or envelope detection schemes. Theoretical analysis and experimental verification are performed. 0.625 Gbaud pre-coded quadrature phase-shift keying or 16 quadrature amplitude modulation signals can both be recovered by power detection without electrical carrier assistance at the receiver after 75 km fiber transmission. Not only robust against the laser phase noise, an improvement of about 5 dB in receiver sensitivity can also be achieved, as compared with the conventional power detection scheme.

*OCIS codes: 060.2330, 060.5625, 060.2840.*
*doi: 10.3788/COL201917.110602.*

Radio over fiber (RoF) enables the synergy between optical fiber communication and wireless access. It has been spotlighted as a promising candidate for next generation fiber-wireless access networks due to its various advantages such as low latency, wide bandwidth, and flexible mobility[1–3]. Based on two light beams and one single-ended photodetector (PD), the optical heterodyne detection (HD) approach can be used for radio frequency (RF) generation[4,5]. It is more attractive in terms of scalability, tunability, and cost-effectiveness for RoF links compared to RF generation in the electrical domain and then driving a wideband electro-optic modulator solution. The HD-based RoF links also provide other advantages, such as providing a considerable coherent gain from the local oscillator (LO) laser to accommodate the splitting losses of distributed optical networks, and enabling finer frequency separation to overcome the demultiplexing bottleneck encountered in ultra-dense wavelength division multiplexing (UDWDM) systems with a channel spacing as low as a few gigahertz, owing to precise tunablity of the LO frequency and the subsequent digital signal processing (DSP).

However, one of the greatest challenges of HD-RoF links is that the generated RF signal suffers phase noise (PN) from the linewidth and relative frequency fluctuation between the two free-running lasers. The PN will undoubtedly induce system performance degradation to RoF links. Many approaches[5–11] have been proposed in the previous research on PN cancellation. When considering RoF downlink, the DSP-based scheme[6,7] may cause the base station (BS) or wireless receiver to be very expensive due to the cost of the analog-digital converter (ADC), especially in high-frequency band wireless applications. This problem can be solved by a square-law-based scheme[5,8–11] such as power detection (also referred to as envelope detection in some literature). However, an electrical carrier along with the information-bearing signal (usually originated from electro-optic modulation operating in the linear region) is indispensable in the traditional power detection method. Since this carrier occupies most of the energy but does not carry any useful information, such a system configuration will not only reduce the power efficiency of both optical and wireless links, but also induce high optical nonlinear effects in RoF-UDWDM scenarios[12].

The signal pre-coding method presented in Refs. [13,14] can be used to solve the aforementioned problems. However, the reported pre-coding-based methods are not transparent to pulse-shaping functions. Moreover, an unexpected electrical carrier will also appear due to the interaction between discontinuous phase distribution and pre-coding operations.

In this Letter, a power-efficient HD-RoF link based on a pre-coding-assisted power detection scheme is presented, the high energy-consuming electrical carrier necessary to conventional power and/or envelope detection schemes can be avoided whilet robust against the PN originated from two unrelated lasers. This scheme has the features of a simple structure for low-cost deployment, a low bandwidth requirement on the electro-optic modulator, and flexibly adjustable RF generation. Furthermore, the proposed scheme is shown to be transparent to pulse-shaping functions and can achieve simultaneous carrierless transmission for both optical and wireless links. In the proof-of-principle experiment, a 0.625 GHz intermediate frequency (IF) signal with 1.25 Gbps for quadrature phase-shift keying (QPSK) or 2.5 Gbps for 16 quadrature amplitude modulation (16-QAM) is first pre-coded at the central station (CS), and then is upconverted to 7.5 GHz RF by optical HD at the BS after a 75 km standard single mode fiber (SSMF) transmission. Finally, power detection is

 

used to downconvert the RF signal while eliminating the PN at the receiver. Meanwhile, the standard vector signal is recovered from the pre-coded signal during this process.

The schematic architecture of the proposed pre-coding-assisted power detection scheme for an RoF link is shown in Fig. 1. At the CS, a carrierless optical signal is generated by performing optical carrier suppression (OCS) modulation on the real-valued pre-coded IF signal. Suppose that the discrete-time standard vector signal is given by

$$c[n] = r_n \exp(j\theta_n), \tag{1}$$

where $r_n$ and $\theta_n$, respectively, are the amplitude and phase of the $n^{\text{th}}$ symbol. For example, $r_n \in \{1\}, \theta_n \in \{0, \pm\pi/2, \pi\}$ for QPSK symbols and $r_n \in \{1, 2\}, \theta_n \in \{0, \pm\pi/4, \pm 2\pi/4, \pm 3\pi/4, \pi\}$ for star 16-QAM symbols, respectively.

Afterward, the information symbols are pulse-shaped by $h_{ps}(t)$. The bandwidth-limited signal after pulse shaping can be expressed as

$$s[t] = \sum_{n=-\infty}^{\infty} c[n] h_{ps}(t - nT) = r(t) \exp\left[j\theta(t)\right], \tag{2}$$

where $T$ is the symbol period, and $r(t)$ and $\theta(t)$ represent the amplitude and phase of the $s[t]$, respectively.

In order to recover the standard vector signal by power detection at the receiver, the above signal should be pre-coded in advance. The pre-coding steps are as follows. First, phase unwrapping[15] is employed to eliminate discontinuous phase distribution. Second, perform the core of pre-coding operation by taking the square root of the amplitude while halving the phase. Hence, the pre-coded baseband signal can be described as

$$s_{pre-coded}(t) = \sqrt{r(t)} \exp\left(j\frac{\theta'(t)}{2}\right), \tag{3}$$

where $\theta'(t) = \theta(t) \pm 2k\pi$ is the unwrapped phase with $k$ taking an integer value. The principle diagram of the pre-coded QPSK signal with and without phase unwrapping is shown in Fig. 2. If the phase-wrapped signal whose phase ranges from $-\pi$ to $\pi$ is a directly performed signal

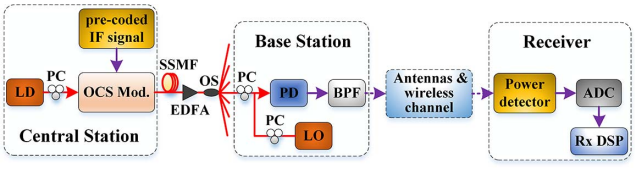


Fig. 1. Schematic architecture of the proposed RoF link based on pre-coding-assisted power detection scheme. LD, laser diode; PC, polarization controller; OCS, optical carrier suppression; Mod, modulation; SSMF, standard single mode fiber; OS, optical splitter; LO, local oscillator; PD, photodetector; BPF, bandpass filter; ADC, analog-digital converter; DSP, digital signal processing. The later experimental setup has been simplified by omitting the wireless transmission link, whilst the BPF and power detection are conducted in digital domain.

pre-coding operation, the corresponding constellation points will only be located in the right-half plane of the in-phase component, because their phases are all constrained between $-\pi/2$ and $\pi/2$. It implies the mean of the pre-coded signal is not zero; that is, a DC component appears that will evolve into an unexpected electrical carrier after frequency upconversion[13,14]. In addition, without phase unwrapping, the phase of the pulse-shaped signal varies over time and has discontinuous phase jumps; i.e., there exists discontinuous phase distribution that consequently leads to spectrum broadening because of the interaction between the discontinuous phase distribution and the pre-coding operation. Fortunately, the above two issues can both be overcome by phase unwrapping prior to signal pre-coding. Therefore, phase unwrapping is a significant and indispensable operation.

Subsequently, the real-valued pre-coded IF signal can be obtained through upconverting baseband to IF as

$$s_{IF}(t) = \sqrt{r(t)} \cos\left(\omega_{IF} t + \frac{\theta'(t)}{2}\right), \tag{4}$$

where $\omega_{IF}$ is the angular frequency of the IF signal. After that, OCS modulation is used for electro-optic conversion. Compared to conventional power detection with non-zero carriers, OCS modulation with pre-coding can obtain a higher power efficiency. Moreover, suppressing the optical carrier can not only improve the power-efficiency of the optical link, but also avoid the conversion from optical carrier to electrical RF tone via HD beating at the BS. Thus, the power-efficiency of the wireless link is also enhanced. For the purpose of concision, OCS modulation is conducted via a dual drive Mach–Zehnder modulator (DD-MZM) biased at its null point in this Letter. Under small signal analysis, the carrierless optical signal can be written as[16]

$$E_s(t) \approx m \cdot s_{IF}(t) \cdot \sqrt{P_c} \exp\left[j(\omega_c t + \varphi_c(t))\right], \tag{5}$$

where $m = \pi / V_\pi$, and $V_\pi$ is the half-wave voltage of the DD-MZM. $P_c$, $\omega_c$, and $\varphi_c(t)$, respectively, are the power, angular frequency, and phase of the lightwave from the transmitter laser.

To meet the requirements of optical distributed networks, the signal light is split and fed to multiple BSs.

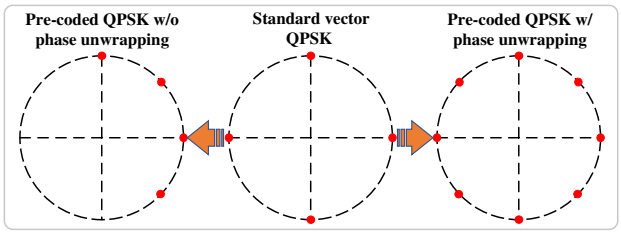


Fig. 2. Principle diagram of the pre-coded QPSK signal with and without phase unwrapping.

At each BS, HD based on a free-running LO laser $E_{LO}(t)$ and a single-ended PD yields a photocurrent $I_{PD}(t)$. For low cost purpose, the LO can be reused from the laser source for uplink transmission[2,17]. The $E_{LO}(t)$ and $I_{PD}(t)$ can be expressed as

$$E_{LO}(t) = \sqrt{P_{LO}} \exp\left[j\left(\omega_{LO}t + \varphi_{LO}(t)\right)\right], \tag{6}$$

$$\begin{aligned} I_{PD}(t) &= R \cdot \left|E_s(t) + E_{LO}(t)\right|^2 \\ &= M \cdot s_{IF}(t)\cos\left(\Delta\omega t + \Delta\varphi(t)\right) \\ &\quad + N \cdot r(t)\cos\left(2\omega_{IF}t + \theta(t)\right) \\ &\quad + N \cdot r(t) + P_{LO}, \end{aligned} \tag{7}$$

where $M = 2mR\sqrt{P_c P_{LO}}$, $N = 0.5m^2RP_c$, and $R$ denotes the responsivity of the PD. $\Delta\omega = \omega_c - \omega_{LO}$ is located in the desired RF band and it supports frequency tunability via a tunable LO laser for different wireless scenarios, and $\Delta\varphi(t) = \varphi_c(t) - \varphi_{LO}(t)$ exhibits the existence of the laser PN. $P_{LO}$, $\omega_{LO}$, and $\varphi_{LO}(t)$ are the power, angular frequency, and phase of the LO light wave, respectively. In Eq. (7), the first term is the pre-coded RF signal, the second term is the decoded IF signal, and the last two terms, respectively, are the DC and interference term. With an appropriate IF assistance, it can easily remove the interference term in the low-pass filtered (LPF) photocurrent to extract the desired IF signal. As can be seen that the obtained IF signal is independent of the laser PN and contains the full transmitted information. It can provide wired services to promote seamless integration of wired and wireless simultaneous access for RoF passive optical networks[18,19]. Since our main purpose in this Letter is to study the PN cancellation for RF band, the IF signal is not the key point to be discussed in subsequent analysis.

For the wireless link, the desired pre-coded RF signal $s_{RF}(t) = M \cdot s_{IF}(t)\cos\left(\Delta\omega t + \Delta\varphi(t)\right)$ can be extracted by a bandpass filter (BPF). However, it still suffers from the PN introduced by the lasers. Ignoring the impacts of the transceiver antennas and wireless channel, the resultant RF signal is then downconverted to IF via a power detector[20] at the wireless receiver. The power detector consists of a square-law device and an LPF. After square-law operation, the output signal of the power detector can be described as

$$\begin{aligned} {s_{RF}}^2(t) &= P \cdot r(t)\cos(2\omega_{IF}t + \theta(t)) + P \cdot r(t) \\ &\quad + P \cdot r(t)[1 + \cos(2\omega_{IF}t + \theta(t))] \\ &\quad \times \cos(2\Delta\omega t + 2\Delta\varphi(t)), \end{aligned} \tag{8}$$

where $P = m^2R^2P_cP_{LO}$. The first two terms are the desired IF signal and undesired interference, respectively. The last term is the high-frequency component, which can be blocked by the LPF of the power detector. Note that $\Delta\varphi(t)$, which represents the laser PN, does not exist in the obtained low-frequency components now. In other words, the robustness against the PN originating from two unrelated lasers in the optic link has been achieved. Then the obtained low-frequency components are sampled and transformed to digital by an ADC. The followed signal processing is done in the DSP module.

The desired signal $s_{rIF}(t) = P \cdot r(t)\cos(2\omega_{IF}t + \theta(t))$ can be extracted by a digital BPF and its frequency has doubled. After downconverting to the baseband and matched filtering by another filter $h_m(t)$ to match the pulse-shaping function $h_{ps}(t)$ for optimal performance, the resultant signal can be expressed as

$$\begin{aligned} s_r(t) &= \left[r(t)\exp\left(j\theta(t)\right)\right] * h_m(t) \\ &= P \cdot \sum_{n=-\infty}^{\infty} c[n]h(t - nT), \end{aligned} \tag{9}$$

where $h(t) = h_{ps}(t) * h_m(t)$ is the overall pulse-shaping function after a convolution operation and is assumed to be a raised cosine function in this Letter. The standard vector signal is then recovered by sampling $s_r(t)$ at the optimum timing points.

In summary, besides reconstructing the standard vector signal from the pre-coded signal, the power detector helps to eliminate the laser PN. Additionally, the power detector also provides a cost-effective frequency downconversion method, especially for a high-frequency band wireless receiver.

A proof-of-principle experiment based on the available components was carried out. The experimental setup followed Fig. 1, with some adjustment. The BPF and power detection were conducted in DSP as well as omitting the wireless transmission link. In MATLAB offline program, 0.625 Gbaud QPSK or 16-QAM signal, was first pulse-shaped by the root raised cosine (RRC) filter. Afterward, the signal was pre-coded after phase unwrapping, and then was upconverted to 0.625 GHz IF in the digital domain. An arbitrary waveform generator (Tektronix AWG70002 A) at a sampling rate of 20 GSa/s, was used to generate the carrierless real-valued pre-coded IF signal. An external cavity laser (ECL) with a 100 kHz linewidth was used as the transmitter laser, producing a continuous wave at 1551.446 nm and a power of 14 dBm. The DD-MZM with a half-wave voltage of about 4 V was biased at its null point to obtain the OCS signal. The attenuation coefficient and dispersion coefficient of the SSMF were 0.2 dB/km and 17 ps/(nm · km), respectively. After a 75 km fiber transmission, the signal light was coupled with a free-running LO laser at 1551.506 nm with a power of 1 dBm, to perform HD based on one single-ended PD (3 dB bandwidth of 10 GHz). A variable optical attenuator was placed before coupling the two light beams to sweep the received optical power (ROP). Finally, the outputs of the PD, including the RF microwave signal with the center frequency of about 7.5 GHz, were directly sampled by an oscilloscope (Tektronix DPO 72504D) operating at 50 GSa/s and processed offline. In the receiver DSP, RF signal filtering, power detection, downconversion to baseband, match filtering, symbol demodulation,

and bit error rate (BER) calculation were performed in sequence.

The experimental results show that there are two key factors affecting the system performance during the pre-coding process. One is the interaction between the discontinuous phase distribution and pre-coding operations, and the other is the sequence of pulse shaping and pre-coding. Figure 3 shows the corresponding spectra of the real-valued pre-coded QPSK IF signal with and without phase unwrapping, respectively, in the case of signal pre-coding after pulse shaping (PCAPS) as demonstrated in the theoretical derivation. Without phase unwrapping, the interaction between the discontinuous phase distribution and pre-coding operation results in an unexpected electrical carrier as well as extra spectrum broadening, as shown in Fig. 3. For comparison, the electrical carrier is eliminated and the spectrum broadening is obviously relieved, when phase unwrapping is used to correct the discontinuous phase. In Fig. 4, we further show the received SNR as the function of the RRC roll-off factor in the PCAPS and signal pre-coding before pulse shaping (PCBPS) cases with and without phase unwrapping, respectively. It can be seen that phase unwrapping can effectively improve the system performance, especially for the PCAPS case. As mentioned above, this should be attributed to the elimination of the electrical carrier and a significant mitigation of spectrum broadening. On the other hand, for the PCBPS case, whose pulse shaping is located between pre-coding and decoding, a larger roll-off factor (not less than 0.5) should be used for better performance. Instead, different roll-off factors can be supported with a flat SNR curve in the PCAPS case. In other words, transparency to pulse-shaping functions has been achieved and highly efficient spectral pulse-shaping functions can be used in this case. Therefore, the PCAPS method is preferred. The following experimental results are also given in this case with phase unwrapping.

The spectrum of the received QPSK signal after the PD is shown as Fig. 5. In the experiment, the IF and RRC roll-off factor, respectively, were set to 0.625 GHz and 0.1. The resultant frequency-doubled IF signal and pre-coded RF signal are found to locate at 1.25 GHz and 7.5 GHz, respectively. After digital BPF and power detection, the pre-coded RF signal is downconverted to IF.

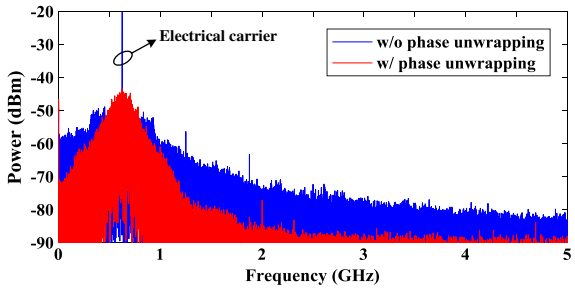


Fig. 3. Spectra of transmitted pre-coded QPSK IF signal with and without phase unwrapping in the signal pre-coding after pulse-shaping case.

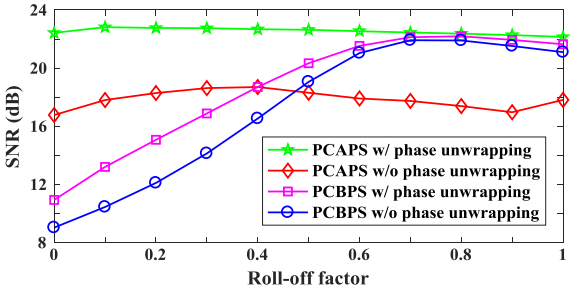


Fig. 4. SNR vs RRC roll-off factor curves for QPSK with and without phase unwrapping using different sequence of pulse shaping and pre-coding. PCAPS, signal pre-coding after pulse shaping; PCBPS, signal pre-coding before pulse shaping.

The digital BPF filter uses an ideal brick-wall filter with a filter bandwidth of 3 GHz, which is sufficient to accommodate the relative frequency drift of the two lasers (up to 120 MHz was found in the experiment). The obtained IF signal, which has a spectrum similar to the low-frequency component given in Fig. 5, is insensitive to the laser PN and decoding from the pre-coded signal has been achieved.

Figure 6 shows 1.25 Gbps QPSK, 2.5 Gbps square, and star 16-QAM BER versus ROP curves for 75 km SSMF transmission without dispersion compensation in the case of two different LO lasers; one is also an ECL laser with 100 kHz linewidth and the other is a distributed feedback (DFB) laser with around 1 MHz linewidth. It is found that the sensitivity penalties of the three modulation formats between the two different linewidths are all less than 0.2 dB at the 7% hard-decision forward error correction (HD-FEC) threshold. These penalties are likely to be due to the causes other than laser linewidth, such as the bias drift of the DD-MZM, and the increase of the relative intensity noise of the LO laser. The receiver sensitivity of QPSK, square and star 16-QAM can achieve around −41.0 dBm, −35.5 dBm, and −34.9 dBm at the 7% HD-FEC threshold, respectively, even using the DFB laser with a linewidth of 1 MHz. The enough margin can well accommodate the splitting losses for optical distribution networks. The corresponding constellation diagrams of QPSK, square and star 16-QAM at the ROP of −25 dBm are depicted as the insets in Fig. 6.

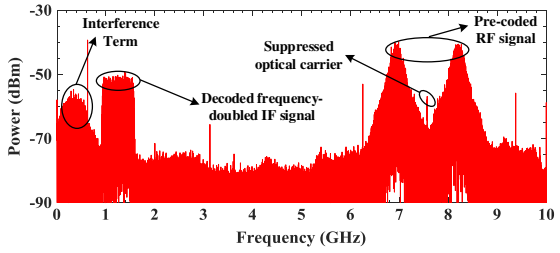


Fig. 5. Spectrum of received QPSK signal with phase unwrapping at the ROP of −2 dBm after the PD. Symbol rate: 625 MSymbol/s; IF center frequency: 0.625 GHz; RF center frequency: 7.5 GHz.

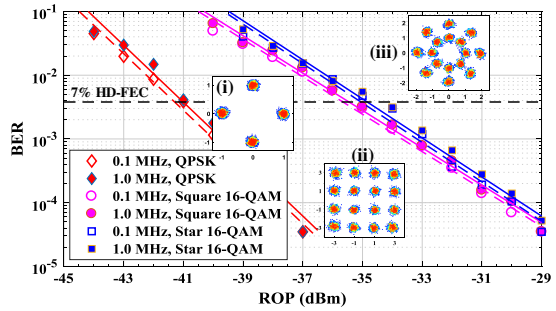


Fig. 6. BER vs ROP curves for 1.25 Gbps QPSK, and 2.5 Gbps square and star 16-QAM signals transmitted over 75 km fiber in the case of two LO lasers with different linewidths. Insets depict the constellation diagrams of (i) QPSK, (ii) square 16-QAM, and (iii) star 16-QAM at the ROP of −25 dBm, respectively.

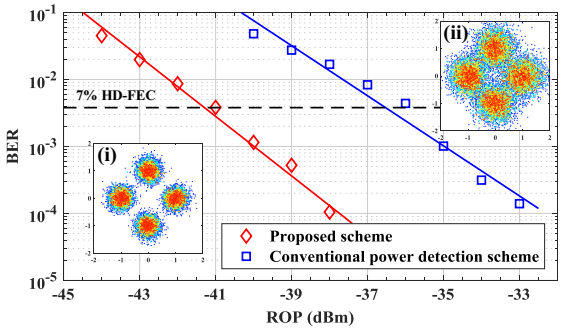


Fig. 7. BER vs ROP performance comparison for QPSK signal between the proposed pre-coding-assisted power detection scheme and conventional power detection scheme after 75 km fiber transmission. Insets (i) and (ii) depict the constellation diagrams of the two schemes at the fixed ROP of −38 dBm, respectively.

In order to further quantify the performance improvement of the proposed scheme, a comparative experiment based on a QPSK signal between the proposed pre-coding-assisted power detection scheme and conventional power detection scheme is performed. The symbol rate, the IF and upconverted RF value, and the power of transmitter laser and LO, as well as the devices used in the experiments are all kept the same. The only difference is that there is no pre-coding process for the conventional power detection scheme and the DD-MZM is biased at the orthogonal point to generate a single sideband signal with the carrier. The corresponding results are shown in Fig. 7. It is found that the proposed scheme has an advantage of about 4.8 dB at the 7% HD-FEC threshold compared to the conventional power detection scheme. This is mainly attributed to its improved power efficiency. The insets in Fig. 7 show the constellation of the two schemes at the fixed ROP of −38 dBm. They noticeably exhibit the performance improvement brought by the proposed scheme.

In conclusion, a power-efficient RoF link based on a pre-coding-assisted power detection scheme has been proposed and experimentally demonstrated. While maintaining superior robustness against the PN resulting from two unrelated lasers, the energy-consuming electrical carrier that is essential to conventional power and/or envelope detection scheme is no longer required. Compared with the conventional power detection scheme, this scheme can bring about 5 dB improvement in receiving sensitivity. It provides a potential candidate for future fiber-wireless access networks, especially in the scene of considering the power budget as a first priority.

This work was supported by the National Natural Science Foundation of China (No. 61420106011) and the Fundamental Research Funds for the Central Universities (No. ZYGX2016J014).

## References

1. J. J. Vegas Olmos, T. Kuri, and K.-i. Kitayama, IEEE Trans. Microwave Theory Tech. **58**, 3001 (2010).
2. C. Liu, L. Zhang, M. Zhu, J. Wang, L. Cheng, and G.-K. Chang, J. Lightwave Technol. **31**, 2869 (2013).
3. Á. Morales, I. T. Monroy, F. Nordwall, and T. Sørensen, Chin. Opt. Lett. **16**, 040603 (2018).
4. I. G. Insua, D. Plettemeier, and C. G. Schäffer, J. Lightwave Technol. **28**, 2289 (2010).
5. O. Omomukuyo, M. P. Thakur, and J. E. Mitchell, IEEE Photon. Technol. Lett. **25**, 268 (2013).
6. Y. Chen, T. Shao, A. Wen, and J. Yao, Opt. Lett. **39**, 1509 (2014).
7. X. Chen and J. Yao, Chin. Opt. Lett. **15**, 010008 (2017).
8. R. Zhang and J. Ma, Opt. Switch. Netw. **25**, 33 (2017).
9. R. Taylor and S. Forrest, J. Lightwave Technol. **17**, 556 (1999).
10. X. Li, Z. Dong, J. Yu, J. Zhang, L. Tao, Y. Shao, and N. Chi, in *Optical Fiber Communication Conference and Exposition and National Fiber Optic Engineers Conference* (2013), paper OW1D.3.
11. H. Wang, L. Yan, J. Ye, B. Luo, W. Pan, X. Zou, and P. Li, Chin. Opt. Lett. **15**, 112301 (2017).
12. T. Kuri and K.-i. Kitayama, J. Lightwave Technol. **21**, 3167 (2003).
13. C.-T. Lin, P.-T. Shih, W.-J. Jiang, E.-Z. Wong, J. J. Chen, and S. Chi, Opt. Lett. **34**, 2171 (2009).
14. X. Chen and J. Yao, J. Lightwave Technol. **34**, 2789 (2016).
15. M. G. Taylor, in *European Conference on Optical Communication* (2005), p. 263.
16. V. C. Duarte, M. V. Drummond, and R. N. Nogueira, J. Lightwave Technol. **34**, 5566 (2016).
17. H. Shams, M. J. Fice, L. Gonzalez-Guerrero, C. C. Renaud, F. van Dijk, and A. J. Seeds, J. Lightwave Technol. **34**, 4786 (2016).
18. H. Kim, T. T. Pham, Y. Won, and S. Han, J. Lightwave Technol. **27**, 2744 (2009).
19. X. Pang, M. Beltrán, J. Sánchez, E. Pellicer, J. J. Vegas Olmos, R. Llorente, and I. T. Monroy, J. Opt. Commun. Netw. **6**, 1 (2014).
20. C. T. Lin, S. C. Chiang, C. H. Li, H. T. Huang, C. H. Lin, and B. J. Lin, Opt. Lett. **42**, 207 (2017).